

# Photoionization of *N*-Alkylphenothiazines in Mesoporous SiMCM-41, AlMCM-41, and TiMCM-41 Molecular Sieves

R. M. Krishna, A. M. Prakash, and Larry Kevan\*

Department of Chemistry, University of Houston, Houston, Texas 77204

Received: September 27, 1999; In Final Form: December 20, 1999

Electron spin resonance and diffuse reflectance spectroscopy have been used to monitor the photoionization yields of *N*-alkylphenothiazine cation radicals ( $PC_n^+$ ) generated by UV irradiation within mesoporous SiMCM-41, AlMCM-41, and TiMCM-41 molecular sieves. Mesoporous SiMCM-41 and AlMCM-41 molecular sieves are efficient for accomplishing stable photoproduced electron transfer of *N*-alkylphenothiazine molecules ( $PC_n$ ) at room temperature and at 77 K. A series of mesoporous TiMCM-41 molecular sieves with variable amounts of framework titanium have been hydrothermally synthesized and used for  $PC_n$  photoionization in comparison with SiMCM-41 and AlMCM-41 molecular sieves. The addition of Ti into the framework of SiMCM-41 increases the net  $PC_n^+$  cation radical photoyield at room temperature and 77 K. Thus, Ti in the TiMCM-41 framework is suggested to act as a better electron acceptor in competition with SiMCM-41 and AlMCM-41 molecular sieves. The photoionization efficiency to form  $PC_n^+$  cation radicals increases in the order SiMCM-41 < AlMCM-41 < TiMCM-41. The photooxidation yields decrease as the alkyl chain lengths of the  $PC_n$  molecules increase from methylphenothiazine ( $PC_1$ ) to hexadecylphenothiazine ( $PC_{16}$ ). Diffuse reflectance (DR) UV–visible spectra support the formation of some radical cation dimer as the alkyl chain length increases from  $PC_1$  to  $PC_{16}$  in all MCM-41 materials and thus the photoionization yields decrease from  $PC_1$  to  $PC_{16}$ . The photoyield is higher by about 2.5 times at 77 K compared to room temperature. The  $PC_n^+$  cation radicals are stable in SiMCM-41, AlMCM-41, and TiMCM-41 at room temperature for several hours and do not decay at 77 K. The observed photoyields of  $PC_n$  molecules in mesoporous MCM-41 molecular sieves suggest that these materials can be utilized effectively for solar energy conversion and storage.

## Introduction

Photoionization is the first step in many light driven reactions related to the storage of light energy.<sup>1</sup> The design of efficient artificial photoredox systems for storing light energy must be able to minimize back electron transfer.<sup>2–4</sup> Heterogeneous systems, such as micelles, vesicles, molecular sieves, layered oxide materials, and silica gel, have been found to be good photoredox systems for solar energy conversion and storage.<sup>1,5–8</sup> Photoionization studies in porous inorganic materials, such as zeolites<sup>6</sup> and silica gels<sup>8</sup> have shown that their cages or pores provide an appropriate microenvironment to retard back electron transfer and increase the lifetime of the photoproduced radical ions. In certain cases photoproduced radical ion lifetimes are stable even at room temperature.<sup>7,8</sup> This has been ascribed to strong electrostatic fields inside such solids.

Photophysical and photochemical reactions in heterogeneous media may differ significantly from analogous reactions in homogeneous solution.<sup>2,9,10</sup> Among the constrained systems utilized to organize reactants, crystalline inorganic solids such as layered materials and zeolites occupy a special position owing to their adsorptive properties, ion exchange ability, and thermal and chemical stability.<sup>11–13</sup> The sizes of zeolite pores enables one to obtain highly efficient charge separation.<sup>14</sup> The effects of the constrained environment on the electronic excited states and reactivities of molecules adsorbed into these porous materials has been studied.<sup>15–18</sup>

In heterogeneous reactions using microporous systems, impeded diffusion of the reagents and accessibility of the sites are limiting factors of importance. In fact, the relatively small

size of the micropores (typically  $\leq 13$  Å) has been claimed as a main drawback for intensive use of zeolites as microscopic reactors.<sup>19</sup> Therefore, it is important to determine the suitability of new zeotypes with larger pore dimensions as hosts to perform photoproduced electron transfer reactions with bulky photoactive molecules. Much effort is currently being devoted to the synthesis of mesoporous M41S molecular sieves to overcome adsorption/diffusion limitations of conventional zeolites.<sup>19</sup>

SiMCM-41 is a mesoporous silica containing a regular array of uniform linear one-dimensional pores with an approximately hexagonal cross section and a diameter from 15 to 100 Å, a high surface area of about 1000 m<sup>2</sup>/g, and a pore size distribution nearly as sharp as that of zeolites.<sup>20,21</sup> The SiMCM-41 materials with these unique properties have promising utility for photo-reactions of bulky molecules in addition to catalysis and separation of large organic molecules. The tetrahedral Si(IV) in the SiMCM-41 framework can be replaced by other metal ions such as Al(III), Ti(IV), Mn(II), and other transition metal ions.<sup>22–24</sup> This makes it possible to modify the SiMCM-41 framework to enhance the photoionization efficiency of incorporated molecules such as *N*-alkylphenothiazines ( $PC_n$ ).

In the present work, we report that the use of SiMCM-41, AlMCM-41, and TiMCM-41 molecular sieves with about 25 Å diameter channels opens new possibilities to carry out efficient photoproduced electron-transfer reactions. This is illustrated here by the incorporation of  $PC_n$  into SiMCM-41, AlMCM-41, and TiMCM-41, which results in a significant increase of the photoyield in the order SiMCM-41 < AlMCM-41 < TiMCM-41. This indicates that framework modification by incorporating

Ti(IV) into SiMCM-41 enhances the electron-accepting ability of the SiMCM-41 framework.

### Experimental Section

**Pure SiMCM-41 Synthesis.** The SiMCM-41 molecular sieve was prepared following the literature procedure.<sup>25</sup> The following chemicals were used without further purification: tetraethyl orthosilicate (TEOS, Aldrich), dodecyltrimethylammonium bromide (DTMABr, TCI) and tetramethylammonium hydroxide (TMAOH, Aldrich, 25%). Deionized water was used throughout the synthesis. Syntheses were carried out in 100 cm<sup>3</sup> stainless steel autoclaves lined with Teflon at autogenous pressure without agitation. In a typical SiMCM-41 synthesis, 10.4 g of TEOS was combined with 11.6 g of DTMABr in 2-propanol under vigorous stirring at room temperature, and then 4.8 g of TMAOH and 76 mL of water were added to the resultant clear solution and stirring was continued for about 2 h. After 2 h of agitation the mixture was heated at 358 K for 4 h to remove 2-propanol and ethanol produced by the hydrolysis of tetraethyl orthosilicate. The resulting gel was crystallized hydrothermally in Teflon-lined autoclaves at 373 K for 7 days. After crystallization the solid product was filtered off, washed with deionized water, and dried in air at 350 K overnight. The material was calcined in air at 820 K for about 6 h to remove the template. The molar composition of the final gel was as follows: 1SiO<sub>2</sub>·0.75DTMABr·0.26TMAOH·84H<sub>2</sub>O.

**Titanium-Containing SiMCM-41 Synthesis.** Titanosilicate mesoporous materials, TiMCM-41, were synthesized as follows. Initially, tetraethyl orthosilicate and the required amount of tetrabutyl orthotitanate (TBOT, Fluka) were vigorously mixed for 30 min and the following synthesis steps were the same as described above for the synthesis of SiMCM-41. The molar composition of the final gel mixture was 1SiO<sub>2</sub>·0.75DTMABr·0.0125TBOT·0.026TMAOH·84H<sub>2</sub>O. These samples are designated as TiMCM-41-(*x*), where *x* is the Si/Ti ratio in the gel. For comparison, impregnated TiO<sub>2</sub>/SiMCM-41 (Si/Ti = 30) was prepared by incipient-wetness impregnation<sup>26</sup> using 0.5 g of ammonium titanyl oxalate. This slurry was stirred for 24 h, dried, and then calcined by raising the temperature slowly to 820 K in flowing air and then keeping the sample at this temperature for 24 h in air.

AlMCM-41 with a Si/Al ratio of 30 in the gel was synthesized according to the literature procedure.<sup>27</sup> Commercial methylphenothiazine designated as PC<sub>1</sub> was received from Aldrich and used as received. *N*-Alkylphenothiazine molecules designated as PC<sub>*n*</sub> (where *n* = 3, 6, 16) were synthesized by earlier literature procedures.<sup>7a,28</sup>

**Characterization.** X-ray powder diffraction patterns were collected on a Philips PW 1840 diffractometer using Cu K $\alpha$  radiation. The diffuse reflectance UV–visible spectra were recorded using a Perkin-Elmer model 330 spectrophotometer with an integrating sphere accessory. Chemical analysis was done on a JEOL JXA-8600 electron microprobe with averaging over several defocused areas to give the bulk composition. Calibration was done with known standards. The ESR spectra were recorded at room temperature and 77 K at X-band frequency using a Bruker ESP 300 spectrometer with 100 kHz field modulation and microwave power low enough to avoid saturation. The photoproduct PC<sub>1</sub><sup>+</sup> or PC<sub>*n*</sub><sup>+</sup> cation radical yields were determined by double integration of the ESR spectra using the ESP 300 software. Each photoyield is an average of three determinations.

For diffuse reflectance measurements the sample was filled into a cylindrical quartz sample cell (20 mm diameter by 1 mm path length) that was evacuated for 2 h and flame-sealed.

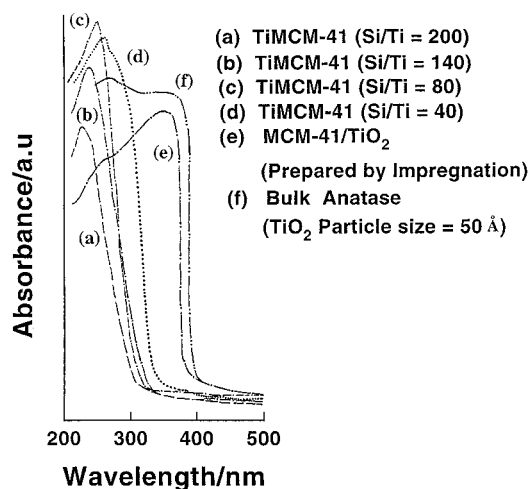


**Figure 1.** Diffuse reflectance UV–visible spectra at room temperature of TiMCM-41-(*x*), where *x* = Si/Ti = 40, 80, 140, 200, impregnated SiMCM-41/TiO<sub>2</sub>, and anatase.

**Samples for Photoionization.** PC<sub>*n*</sub> was incorporated into SiMCM-41, AlMCM-41, and TiMCM-41 by impregnation. For impregnation, 0.5 g of each MCM-41 sample was immersed in 2 mL of 10<sup>−2</sup> M PC<sub>*n*</sub>/C<sub>6</sub>H<sub>6</sub> solution overnight, and then all the solvent was removed by flowing nitrogen through the samples for about 3 h. Thus, all samples contained the same amount of PC<sub>*n*</sub>. For ESR measurements the same amount (~20 mm in height) of impregnated dried powders was placed into 2 mm i.d. by 3 mm o.d. Suprasil quartz tubes, evacuated below 1 Torr for 6 h at room temperature and sealed. All the samples were prepared in the dark to minimize exposure to visible light.

The evacuated MCM-41/PC<sub>*n*</sub> samples were irradiated with a 300 W Cermox xenon lamp (ILC-LX 300 UV) at room temperature and 77 K. The light was passed through a 10 cm water filter and a Corning No. 7-51 glass filter, which passes light of wavelength longer than 320 nm. For more homogeneous irradiation of the samples, each sample was irradiated in a quartz dewar that was rotated at 4 rpm at room temperature and 77 K. The photoinduced PC<sub>1</sub><sup>+</sup> or PC<sub>*n*</sub><sup>+</sup> radical cations were identified by ESR and DR UV–visible spectroscopy.

### Results

X-ray diffraction patterns of both as-synthesized and calcined SiMCM-41, AlMCM-41, and TiMCM-41 samples match the literature.<sup>22,29</sup> No impurity phases were detected. The diffuse reflectance UV–visible spectra of the TiMCM-41-(*x*) samples are shown in Figure 1. Compared to bulk anatase (about 50 Å diameter TiO<sub>2</sub> particles), the absorption edges of the TiMCM-41 samples are blue-shifted by over 50 nm. The TiMCM-41 samples of low titanium content (Si/Ti ≥ 80) show absorption bands centered near 220–250 nm, which can be assigned to a ligand-to-metal charge-transfer transition between the oxygen ligands to tetrahedral coordinated Ti(IV) ions.<sup>30,31</sup> This indicates that the Ti(IV) ions are incorporated into the framework of MCM-41.<sup>22</sup> The spectra of TiMCM-41 show no prominent absorption band at 300–350 nm, which suggests that a segregated crystalline TiO<sub>2</sub> phase-like anatase is absent in TiMCM-41. But, TiMCM-41-(40) of higher Ti content shows a broad, red-shifted absorption band at 220–350 nm compared to TiMCM-41 with lower Ti contents. The red shift is more significant in TiMCM-41-(40). This indicates that a part of titanium in these materials is in octahedral coordination similar to that in TiO<sub>2</sub> particles. These results are consistent with previous characterization results<sup>22,29,32</sup> of TiMCM-41 samples with different Ti contents.

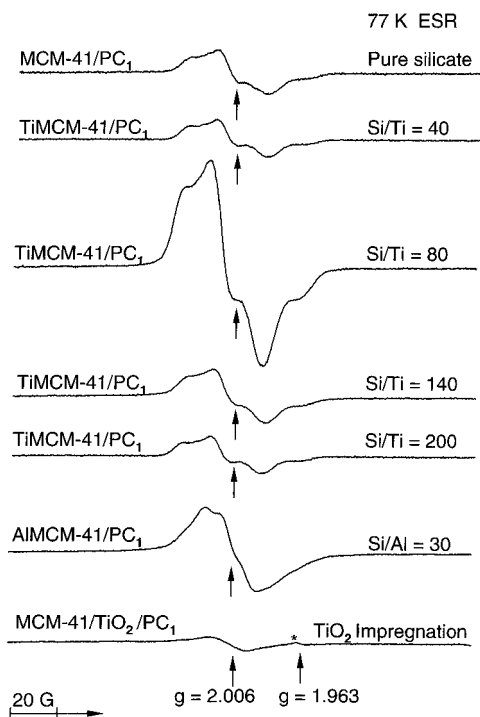


**Figure 2.** ESR spectra at 77 K of SiMCM-41/PC<sub>1</sub>, TiMCM-41-(x)/PC<sub>1</sub>, where  $x = \text{Si/Ti} = 40, 80, 140, 200$ , AIMCM-41/PC<sub>1</sub>, and SiMCM-41/TiO<sub>2</sub>/PC<sub>1</sub> samples after 60 min room-temperature photoirradiation at 320 nm.

After removal of the organic template by calcination in air at 820 K, SiMCM-41, AIMCM-41, and TiMCM-41-(x) showed no ESR signal at room temperature or 77 K. However, samples of SiMCM-41, AIMCM-41, and TiMCM-41 impregnated with PC<sub>1</sub> show very weak ESR signals of PC<sub>1</sub><sup>+</sup> cation radicals based on  $g = 2.006$  with incompletely resolved hyperfine coupling<sup>33</sup> before photoirradiation. These samples without PC<sub>1</sub> give no ESR signals after photoirradiation. This indicates that some PC<sub>1</sub><sup>+</sup> cation radicals are produced during the preparation of samples. The color of the samples only changed to very light pink after PC<sub>1</sub> impregnation, indicating less dark reaction. The samples showed much stronger ESR signals at  $g = 2.006$  at room temperature after being irradiated by 320 nm light at room temperature<sup>8</sup> for 60 min, and the color of the samples turns deep pink, which is characteristic of PC<sub>1</sub><sup>+</sup> cation radicals.<sup>7,8,33,34</sup> This indicates photoinduced formation of PC<sub>1</sub><sup>+</sup> cation radicals at room temperature in SiMCM-41, AIMCM-41, and TiMCM-41 samples. The low loadings (0.01 M) of PC<sub>n</sub> molecules correspond to optimal photoyields of about 15–20% of the PC<sub>n</sub> based on optical absorption. The 0.01 M loading corresponds to about 2% coverage of the surface area of the MCM-41 channels. If the loadings are increased, the photoyield decreases. The photoyield at 77 K is about 2.5 times greater than at room temperature, as shown in Figures 2 and 3. PC<sub>1</sub><sup>+</sup> cation radicals are stable at room temperature and do not decay at 77 K in all MCM-41 samples. Figures 4 and 5 show that the PC<sub>1</sub><sup>+</sup> cation radical photoyield is greatest in TiMCM-41 in comparison with SiMCM-41 and AIMCM-41. The photoyield in TiMCM-41 increases with increasing Ti content in TiMCM-41, as shown in Figure 5 with different photoirradiation times. The photoyield increases up to a Si/Ti ratio of 80 in the gel and then decreases for a Si/Ti ratio of 40 in the gel, as shown in Figure 5. The Si/Ti ratios of the gel mixtures and the corresponding solid products are as follows: 200 gel → 99, 140 gel → 61, 80 gel → 49, and 40 gel → 24. The enhancement of the photoyield in TiMCM-41 is discussed below.

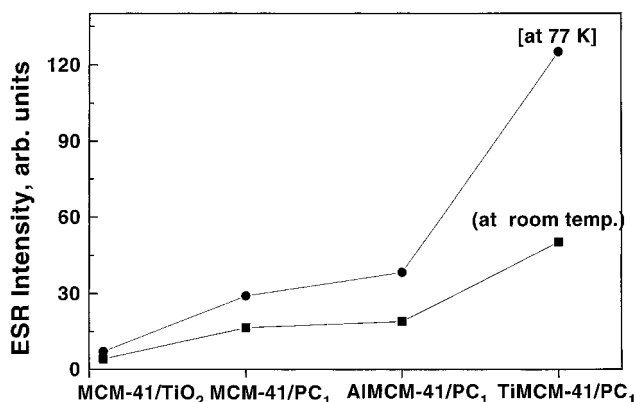


**Figure 3.** PC<sub>1</sub><sup>+</sup> photoyields in SiMCM-41, AIMCM-41, TiMCM-41-(80), and MCM-41/TiO<sub>2</sub> after 60 min photoirradiation with 320 nm at room temperature and at 77 K.

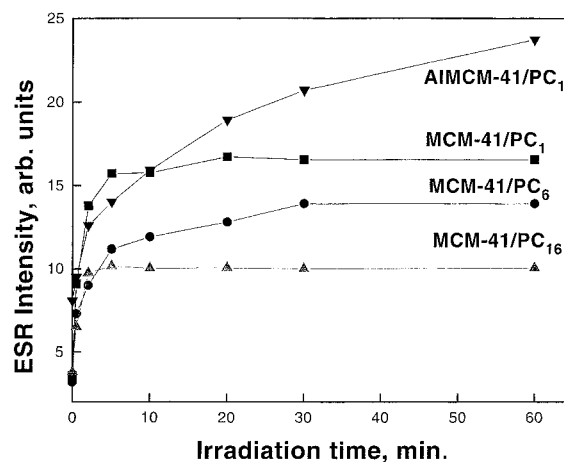


**Figure 4.** PC<sub>n</sub><sup>+</sup> photoyields of SiMCM-41/PC<sub>1</sub>, SiMCM-41/PC<sub>6</sub>, SiMCM-41/PC<sub>16</sub>, and AIMCM-41/PC<sub>1</sub> measured by ESR at room temperature after 60 min room-temperature photoirradiation at 320 nm.

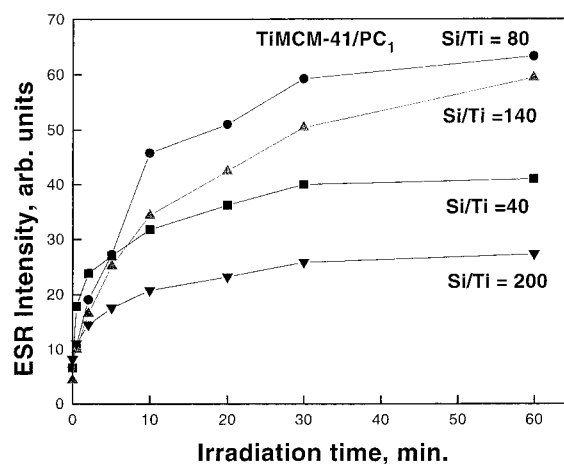


**Figure 5.** PC<sub>1</sub><sup>+</sup> photoyields at room temperature versus 320 nm photoirradiation time for TiMCM-41-(x) where  $x = \text{Si/Ti} = 40, 80, 140, 200$ .

The effects on the photoyield of PC<sub>n</sub><sup>+</sup> cation radicals as the alkyl chain length changes from 1 to 16 carbons in SiMCM-41 and TiMCM-41 samples are shown in Figures 6 and 7 at room temperature. The diameters of PC<sub>1</sub>, PC<sub>3</sub>, PC<sub>6</sub>, and PC<sub>16</sub> molecules are about 6.5, 7.8, 10.5, and 20 Å, respectively. From Figures 6 and 7, one can observe that the photoyields decrease with increasing alkyl chain length. The stability of the PC<sub>1</sub><sup>+</sup> cation radicals increases from PC<sub>1</sub> to PC<sub>16</sub> in SiMCM-41, AIMCM-41, and TiMCM-41 samples from a few hours to

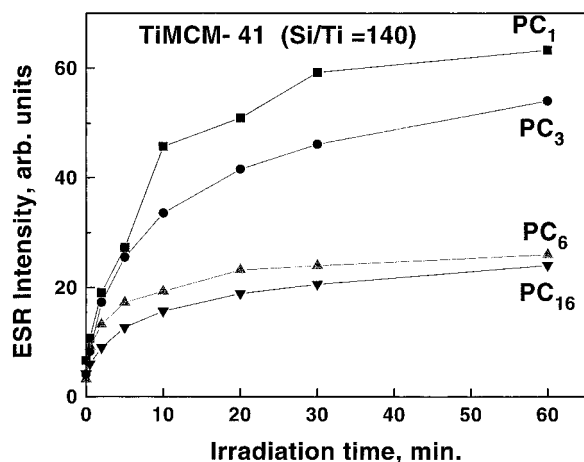


**Figure 6.**  $PC_n^+$  photoyields of TiMCM-41-(140)/ $PC_n$ , where  $n = 1, 3, 6, 16$ , measured by ESR at room temperature after 60 min photoirradiation with 320 nm at room temperature versus the alkyl chain length of  $PC_n$ .

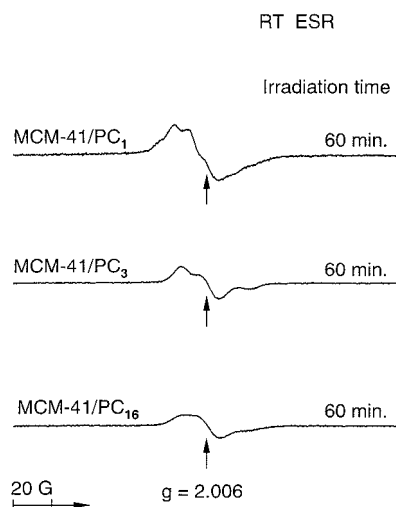


**Figure 7.** ESR spectra at room temperature of SiMCM-41/ $PC_n$ , where  $n = 1, 3, 16$ , samples after 60 min room-temperature photoirradiation at 320 nm.

several days. Thus, the photoyield and stability of the  $PC_1^+$  cation radicals are affected by changing the alkyl chain length from 1 to 16 carbons. The ratio of initial slopes for  $PC_1^+$  cation radical production in TiMCM-41 is almost 20 times that of  $PC_1^+$  cation radical production in SiMCM-41 and AIMCM-41. Assuming first-order kinetics, the initial growth rates are  $1 \times 10^{-1} \text{ s}^{-1}$  for TiMCM-41,  $4 \times 10^{-2} \text{ s}^{-1}$  for AIMCM-41, and  $5 \times 10^{-2} \text{ s}^{-1}$  for SiMCM-41.

The ratio of the initial slopes for  $PC_1^+$  cation radical decay in TiMCM-41 is about 2 times that in SiMCM-41 and AIMCM-41. Assuming first-order kinetics, the initial decay rates are  $1.5 \times 10^{-3} \text{ s}^{-1}$  for TiMCM-41,  $4.0 \times 10^{-3} \text{ s}^{-1}$  for SiMCM-41, and  $3.8 \times 10^{-3} \text{ s}^{-1}$  for AIMCM-41.

The ESR spectral resolution and line width depend on the mobility of the radical.<sup>7,8,33</sup> The partially resolved ESR spectra of the  $PC_1^+$  cation radicals (Figure 2) show that the radicals have some mobility in the SiMCM-41, AIMCM-41, and TiMCM-41 channels. The mobility of the alkylphenothiazine cation radicals may depend on the channel sizes. For large channels (silica gel) a greater mobility correlates with smaller net photoyields, whereas for small channels (MCM-41, zirconium phosphate, ETS-10) a lower mobility correlates with higher net photoyields.

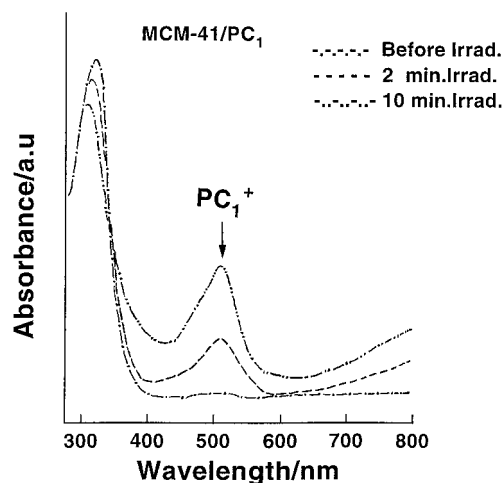


**Figure 8.** UV-visible diffuse reflectance spectra of SiMCM-41/ $PC_1$  samples at room temperature before photoirradiation and after different room-temperature photoirradiation times at 320 nm.

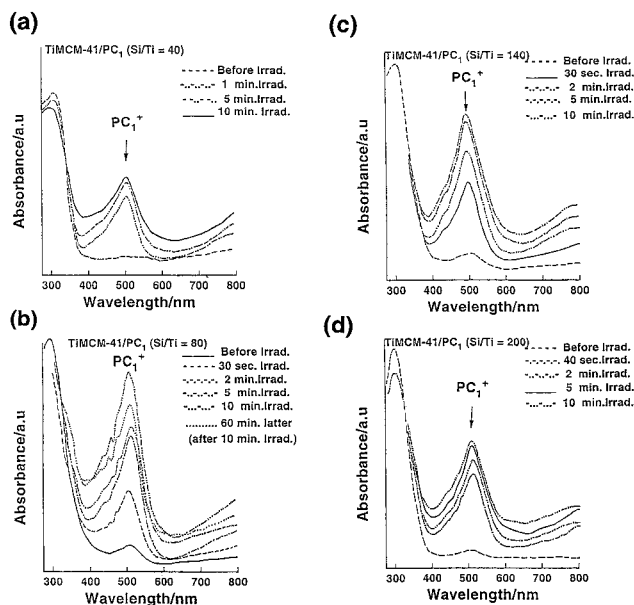


**Figure 9.** UV-visible diffuse reflectance spectra of TiMCM-41-( $x$ )/ $PC_1$ , where  $x = \text{Si/Ti} = 40, 80, 140, 200$ , samples at room temperature before photoirradiation and after different room-temperature photoirradiation times at 320 nm.

Figures 8–11 show the diffuse reflectance spectra of impregnated SiMCM-41/ $PC_1$ , TiMCM-41-( $x$ )/ $PC_1$ , where  $x = 40, 80, 140, 200$ , TiMCM-41-(80)/ $PC_3$ , TiMCM-41-(80)/ $PC_{16}$ , and SiMCM-41/ $\text{TiO}_2$ / $PC_1$  samples before photoirradiation and after photoirradiation at room temperature for different times. Before photoirradiation the spectrum shows strong absorption in the UV region, which is attributed to  $PC_n$  (where  $n = 1, 3, 16$ ) molecules in SiMCM-41 and TiMCM-41. After different UV irradiation times at room temperature the samples turn deep pink and the absorption spectrum in the visible range is the same as the absorption spectrum of  $PC_1^+$  cation radicals in silica gels, layered materials, and microporous materials.<sup>7a,8,33</sup> Similar spectral changes are observed in the DR UV-visible spectra of AIMCM-41/ $PC_n$  samples. This indicates that some stable  $PC_1^+$  cation radicals are generated by UV irradiation and the data confirms the conversion of  $PC_n$  molecules into  $PC_n^+$  cation radicals in SiMCM-41, AIMCM-41, and TiMCM-41. Following photolysis, the spectra (Figures 10 and 11) show strong absorption bands between 600 and 800 nm and are assigned with some uncertainty to some amount of radical cation dimer



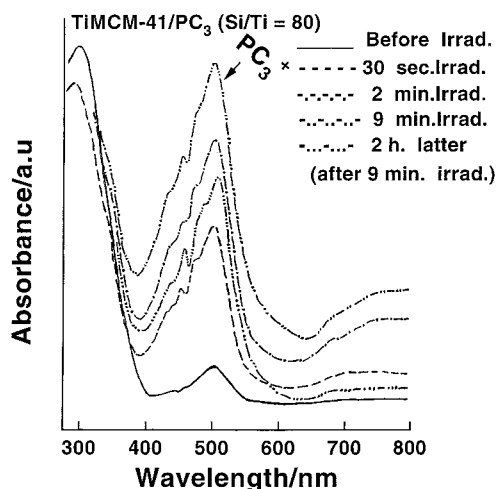


**Figure 10.** UV-visible diffuse reflectance spectra of TiMCM-41-(80)/PC<sub>3</sub> at room temperature before photoirradiation and after different room-temperature photoirradiation times at 320 nm.

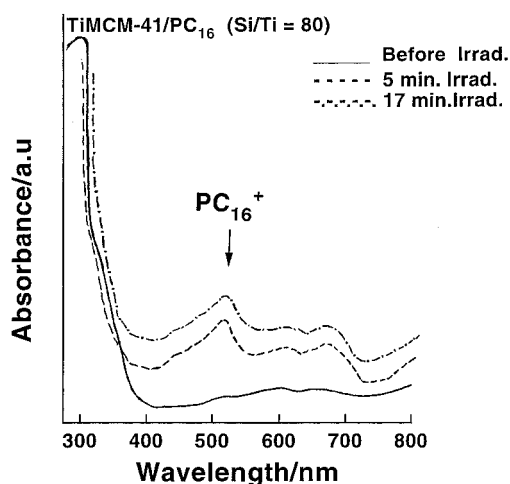


**Figure 11.** UV-visible diffuse reflectance spectra of TiMCM-41-(80)/PC<sub>16</sub> at room temperature before photoirradiation and after different room-temperature photoirradiation times at 320 nm.

(PC<sub>n</sub>)<sub>2</sub>.<sup>35</sup> At room temperature, the half-life of photoproduct PC<sub>1</sub><sup>+</sup> cation radicals in SiMCM-41, AIMCM-41, and TiMCM-41 samples are about 1, 2, and 4 h, respectively.

## Discussion

Phenothiazine and alkylphenothiazine are known to undergo slow oxidation by single electron steps in solution into their respective cation radicals.<sup>7a,36</sup> In the present work, when the PC<sub>n</sub> alkyl chain length is short, some of the PC<sub>n</sub> molecules react with the atmospheric oxygen during sample preparation, oxidize, and turn light pink. Increasing the alkyl chain length of the PC<sub>n</sub> molecules reduces the extent of this dark reaction with atmospheric oxygen, although the reason for this trend is not understood.

Figure 2 shows the ESR signals of PC<sub>1</sub><sup>+</sup> cation radicals in SiMCM-41, AIMCM-41, and TiMCM-41-(x), based on  $g = 2.006$  with incompletely resolved hyperfine coupling, after 60 min irradiation 77 K. The 77 K PC<sub>1</sub><sup>+</sup> cation radical photoyields in SiMCM-41, AIMCM-41 and TiMCM-41-(x) (Figures 3) are about 2.5 times greater than those at room temperature. This can be explained by the lack of much PC<sub>1</sub><sup>+</sup> cation radical mobility at 77 K, which hinders back electron transfer to the PC<sub>1</sub> molecules and thus increases the photoyield. In the other

work,<sup>8</sup> PC<sub>1</sub> molecules incorporated into silica gel show higher photoyields at 77 K than at room temperature.

The ESR and diffuse reflectance results clearly confirm the photooxidation of PC<sub>n</sub> molecules into PC<sub>n</sub><sup>+</sup> cation radicals in MCM-41 materials by UV irradiation. The MCM-41 framework is the likely electron acceptor and may involve surface hydroxy groups. In other works, the surface hydroxy groups on silica gel have been suggested to act as an electron acceptor to form hydrogen atoms that are stably trapped at 77 K in silica gel and detected by ESR.<sup>8</sup> The hydrogen atom signal intensity decreases with smaller pore size.<sup>8</sup> Since MCM-41 has a small pore size ( $\sim 25$  Å), the lack of trapped hydrogen atoms is consistent with these earlier studies on silica gel<sup>8</sup> and layered ZrP.<sup>7a</sup> However, the framework modification by incorporating metal ions into SiMCM-41 enhances the electron-accepting ability of the SiMCM-41 framework.

PC<sub>1</sub>/TiMCM-41-(x) has the highest photoyield when compared to SiMCM-41 and AIMCM-41. The photoyield increases as the Ti content increases in TiMCM-41-(x) to a Si/Ti ratio of 80 and then decreases at a Si/Ti ratio of 40, as shown in Figure 5. The decrease in the PC<sub>1</sub><sup>+</sup> cation radical photoyield in TiMCM-41 for a Si/Ti ratio of 40 is due to the lack of framework incorporation of all the Ti and also the presence of a fraction of TiO<sub>2</sub> particles.<sup>29,32</sup> PC<sub>1</sub> impregnated TiO<sub>2</sub>-SiMCM-41 (Si/Ti = 30) shows no photoyield enhancement due to TiO<sub>2</sub> addition and also the photoyield is much lower than in SiMCM-41, as shown in Figures 2 and 3. The TiO<sub>2</sub> particles in impregnated TiO<sub>2</sub>-SiMCM-41 seem to be too large to be dispersed inside the 25 Å SiMCM-41 pores, and most of the TiO<sub>2</sub> particles are probably located outside the SiMCM-41 pores and block the pores to result in a lower PC<sub>1</sub><sup>+</sup> cation radical photoyield compared to that in SiMCM-41 (Figures 2 and 3).

The photoyield of PC<sub>n</sub><sup>+</sup> cation radicals decreases as the alkyl chain length increases in SiMCM-41 and TiMCM-41 from PC<sub>1</sub> to PC<sub>16</sub>, as shown in Figures 6 and 7. A possible model for this trend is as follows. When the PC<sub>n</sub> alkyl chain length is short (PC<sub>1</sub>), all the PC<sub>1</sub> are distributed uniformly within the pores of the MCM-41 materials and the photooxidation yields are high (Figures 4 and 5). Thus, the decreased photooxidation yields for SiMCM-41/PC<sub>n</sub><sup>+</sup> and TiMCM-41/PC<sub>n</sub><sup>+</sup> may suggest that as the alkyl chain length increases, the PC<sub>n</sub> become distributed more nonuniformly inside the pores of MCM-41, which makes oxidation less efficient.<sup>7a,37</sup> In the other work, *N*-alkylphenothiazine molecules with longer alkyl chain lengths show decreased reactivity toward oxidizing agents.<sup>38</sup> Diffuse reflectance UV-visible spectra (Figures 10 and 11) of TiMCM-41-(80)/PC<sub>3</sub> and TiMCM-41-(80)/PC<sub>16</sub> suggest the formation of clusters as the alkyl chain length increases from PC<sub>1</sub> to PC<sub>16</sub>. However, the stability of the PC<sub>n</sub><sup>+</sup> cation radicals increases from PC<sub>1</sub> to PC<sub>16</sub>. This increase in stability can be explained in terms of an increased inductive effect in PC<sub>1</sub><sup>+</sup> cation radicals as a function of longer alkyl chain length.<sup>7a,33,39</sup>

The higher PC<sub>1</sub><sup>+</sup> cation radical photooxidation yields and slower radical decay in TiMCM-41 compared to SiMCM-41 and AIMCM-41 suggest that TiMCM-41 is a better electron acceptor than AIMCM-41 or SiMCM-41 presumably due to reduction of Ti(IV) in the framework. Earlier, it has been shown that surface Ti(IV) sites in TiMCM-41 immobilize vanadium species and promote oxidation of VO<sup>2+</sup> to V<sup>5+</sup>, probably due to the reducibility of Ti(IV) to Ti(III) in TiMCM-41.<sup>26</sup> Similarly, the photoionization of PC<sub>n</sub> molecules in TiMCM-41 results in a higher PC<sub>1</sub><sup>+</sup> cation radical photoyield and slower radical decay compared to AIMCM-41 or SiMCM-41. So, it is suggested that Ti(IV) sites in TiMCM-41 act as electron acceptor sites.<sup>29,31</sup>

One can expect to see an ESR signal of Ti(III) species<sup>32</sup> produced by photoelectron transfer from PC<sub>n</sub>, but this is not detected at 77 K possibly due to overlap with the PC<sub>1</sub><sup>+</sup> cation radical ESR signal. Overall, it looks like Ti(IV) in TiMCM-41 acts as an electron acceptor site to increase the photoyield of PC<sub>1</sub><sup>+</sup> cation radicals and that the decay rate of PC<sub>1</sub><sup>+</sup> cation radicals is also decreased in TiMCM-41. We are currently investigating photooxidation of PC<sub>n</sub><sup>+</sup> in MCM-41 materials by incorporating other transition metal ions. The photooxidation of PC<sub>n</sub><sup>+</sup> cation radicals in mesoporous MCM-41 materials is more efficient than in silica gel and less efficient than in zirconium phosphate and microporous ETS-10 for similar molecules with similar loadings.

## Conclusions

The photoionization of *N*-alkylphenothiazine molecules incorporated in mesoporous MCM-41 molecular sieves is studied with 320 nm light irradiation at room temperature and 77 K. Mesoporous MCM-41 molecular sieves with incorporated PC<sub>n</sub> molecules are found to be promising hosts for stable photoinduced charge separation. The photoyield and stability of PC<sub>n</sub><sup>+</sup> cation radicals depends on the alkyl chain length. The PC<sub>n</sub><sup>+</sup> cation radical photoyield increases in the order SiMCM-41 < AlMCM-41 < TiMCM-41. The photoyield is about 2.5 times higher at 77 K than at room temperature. As the Ti content increases in TiMCM-41/PC<sub>n</sub>, the PC<sub>1</sub><sup>+</sup> cation radicals decay more slowly. The Ti(IV) sites in the TiMCM-41 framework enhance the electron-accepting ability of the framework, probably due to the reduction of Ti(IV) to Ti(III). These results clearly highlight the utility of mesoporous MCM-41 materials in controlling photoprocesses of PC<sub>n</sub> molecules by incorporating redox metal ions into MCM-41.

**Acknowledgment.** This research was supported by the Division of Chemical Sciences, Office of Basic Energy Sciences, Office of Energy Research, U.S. Department of Energy and by the Texas Advanced Research Program.

## References and Notes

- (1) Kevan, L. In *Photoinduced Electron-Transfer Part B*; Fox, M. A., Chanon, M., Eds.; Elsevier: Amsterdam, 1988; p 329.
- (2) *Photochemical Conversion and Storage of Solar Energy*; Connolly, J. S., Ed.; Academic: New York, 1981; pp 97, 297.
- (3) Vermeulen, L. A.; Thompson, M. E. *Nature* **1992**, 358, 656.
- (4) Thomas, J. K. *Chem. Rev.* **1993**, 93, 301.
- (5) Hurst, J. K.; Lee, L. Y. C.; Gratzel, M. J. *J. Am. Chem. Soc.* **1983**, 105, 7048.
- (6) (a) Corma, A.; Fornes, V.; Garcia, H.; Miranda, M. A.; Sabater, M. J. *J. Am. Chem. Soc.* **1994**, 116, 9767. (b) Gener, I.; Buntinx, G.; Bremard, C. *Angew. Chem., Int. Ed. Engl.* **1999**, 38, 1819. (c) Borja, M.; Dutta, P. K. *Nature* **1993**, 362, 43. (d) Ledney, M.; Dutta, P. K. *J. Am. Chem. Soc.* **1995**, 117, 7687.
- (7) (a) Krishna, R. M.; Kurshev, V.; Kevan, L. *Phys. Chem. Chem. Phys.* **1999**, 1, 2833. (b) Krishna, R. M.; Kevan, L. *Microporous Mesoporous Mater.* **1999**, 32, 169.
- (8) (a) Xiang, B.; Kevan, L. *Langmuir* **1994**, 10, 2688. (b) Xiang, B.; Kevan, L. *J. Phys. Chem.* **1994**, 98, 5120.
- (9) Ramamurthy, V. *Photochemistry in Organized and Constrained Media*; VCH: New York, 1991.
- (10) *Photochemistry on Solid Surfaces*; Anpo, M., Matsura, T., Eds.; Studies in Surface Science and Catalysis, Vol. 47; Elsevier: Amsterdam, 1989.
- (11) O'Hare, D. In *Inorganic Materials*; Bruce, D. W., O'Hare, D., Eds.; Wiley: Chichester, U.K., 1992; Chapter 4.
- (12) *Intercalation Chemistry*; Whittingham, M. S., Jacobson, A. J., Eds.; Academic Press: New York, 1982; p 101.
- (13) Barrer, R. M. *Zeolites and Clay Minerals as Sorbents and Molecular Sieves*; Academic Press: London, 1978; Chapters 1, 2.
- (14) Yoon, K. B. *Chem. Rev.* **1993**, 93, 321.
- (15) Anpo, M.; Yamashita, H.; Zhang, S. *Curr. Opin. Solid State Mater. Sci.* **1996**, 1, 219.
- (16) Anpo, M.; Nishiguchi, H.; Fujii, T. *Res. Chem. Intermed.* **1990**, 13, 73.
- (17) *Surface Photochemistry*; Anpo, M., Ed.; Wiley: London, 1996.
- (18) Nishiguchi, H.; Yukawa, K.; Yamashita, H.; Anpo, M. *J. Photochem. Photobiol. A* **1995**, 99, 1.
- (19) Davis, M. E. *Acc. Chem. Res.* **1993**, 26, 111.
- (20) Kresge, C. T.; Leonowicz, M. E.; Roth, W. J.; Vartuli, J. C.; Beck, J. S. *Nature* **1992**, 359, 710.
- (21) Stuckey, G. D.; Monnier, A.; Schuth, F.; Hou, Q.; Margolese, D.; Kumar, D.; Kridhamurthy, M.; Petroft, P.; Firouzi, A.; Janicke, M.; Chmelka, B. F. *Mol. Cryst. Liq. Cryst.* **1994**, 240, 187.
- (22) Alba, M. D.; Luan, Z.; Klinowski, J. *J. Phys. Chem.* **1996**, 100, 2179.
- (23) Zhao, D.; Goldfarb, D. *J. Chem. Soc., Chem. Commun.* **1995**, 875.
- (24) Tuel, A. *Zeolites* **1995**, 15, 228.
- (25) Koyano, K. A.; Tatsumi, T. *Microporous Mater.* **1997**, 10, 259.
- (26) Luan, Z.; Kevan, L. *J. Phys. Chem. B* **1997**, 101, 2020.
- (27) Luan, Z.; Cheng, C.-F.; Zhou, W.; Klinowski, J. *J. Phys. Chem.* **1995**, 99, 1018.
- (28) Gozlan, I.; Ladkani, D.; Halpern, M.; Rabinovitz, M.; Anoir, D. *J. Heterocycl. Chem.* **1984**, 21, 613.
- (29) Sung-Suh, M. H.; Luan, Z.; Kevan, L. *J. Phys. Chem. B* **1997**, 101, 10455.
- (30) Maschmeyer, T.; Rey, F.; Sankar, G.; Thomas, J. M. *Nature* **1995**, 378, 159.
- (31) Notari, B. *Adv. Catal.* **1996**, 41, 258.
- (32) Prakash, A. M.; Sung-Suh, M. H.; Kevan, L. *J. Phys. Chem. B* **1998**, 102, 857.
- (33) Krishna, R. M.; Prakash, A. M.; Kurshev, V.; Kevan, L. *Phys. Chem. Chem. Phys.* **1999**, 1, 4119.
- (34) Hovey, M. C. *J. Am. Chem. Soc.* **1982**, 104, 4196.
- (35) Yida, Y. *Bull. Chem. Soc. Jpn.* **1971**, 44, 663.
- (36) Braun, A. M.; Gilson, M.-A.; Krieg, M.; Maurett, M.-T.; Murasecco, P.; Oliveros, E. In *Organic Phototransformations in Non-Homogeneous Media*; Fox, M. A., Ed.; ACS Symposium Series 278; American Chemical Society: Washington, DC, 1985; p 79.
- (37) Louis, L.; Tozer, T. N.; Tuck, L. D.; Loveland, D. B. *J. Med. Chem.* **1972**, 15, 898.
- (38) Pelizzetti, E.; Mentasi, E. *Inorg. Chem.* **1979**, 18, 583.
- (39) Levitt, L. S.; Widing, H. F. In *Progress in Physical Organic Chemistry*; Taft, R. W., Ed.; Wiley: New York, 1976; Vol. 12, Chapter 5.